Estimation and Modelling the pre-monsoon Aerosol Optical depth over the Indian Subcontinent: Implication to dust and anthropogenic contribution

Vhanbatte Shrinish Rajesh

19CE36022

Estimation and Modelling pre-monsoon aerosol optical depth over the Indian subcontinent: Implication to dust and anthropogenic contribution

M.Tech Project submitted to the

Indian Institute of Technology Kharagpur

For the partial fulfilment of the degree of

Master of Technology

by

Vhanbatte Shrinish Rajesh
Roll No: 19CE36022

Under the guidance of

Prof. Shubha Verma

Department of Civil Engineering

Indian Institute of Technology Kharagpur
November 2023

©2023 Vhanbatte Shrinish. All rights reserved.

DECLARATION

I hereby declare that this M. Tech Project entitled “Estimation and Modelling pre-monsoon aerosol optical depth over the Indian subcontinent: Implication to dust and anthropogenic contribution”.

I declare that work contained in this project has been done by me under the guidance of my supervisor. I have adequately cited and referenced the original sources.

I also declare that I have conformed to the norms and guidelines given in the Ethical Code of Conduct of the Institute

Vhanbatte Shrinish

19CE3602

CERTIFICATE

This is to certify that the project entitled, ”Estimation and Modelling pre-monsoon aerosol optical depth over the Indian subcontinent: Implication to dust and anthropogenic contribution” submitted by Vhanbatte Shrinish (19CE36022) to the Indian Institute of Technology Kharagpur, for partial fulfillment of the award of the degree of Master of Technology in Environmental Engineering and Management, is a record to bonafide research work carried under my supervision. The contents embodied in this thesis have not been submitted to any other university or institute for the award of any degree or diploma.

Prof. Shubha Verma
(Supervisor)
Department of Civil Engineering
Indian Institute of Technology
Kharagpur-721302, India

Date:
Place: Kharagpur

ACKNOWLEDGEMENT

The work as described in this treatise would not have materialized without the support that I have received from different persons around me.

To start with, I am indebted to Dr. Shubha Verma, my Masters supervisor who had believed in me and guided me throughout. Her resolute attitude and intellect has given me the strength to take over this work through thick and thin. She has constantly persuaded me to refine my analysis to a finer degree and thus bring out the best out of this research work. I am grateful to her for guiding me in right path.

I would take this opportunity to thank the Head of the Department Prof. Dr. Nirjhar Dhang, whose positive attitude has always been an inspiration to me. This moment also calls for thanking Dr. Anjali Pal, Dr. Ashok Kumar Gupta, Dr. Brajesh Kumar Dubey, Dr. Makarand Madhao Ghangrekar and Dr. Sudha Goel, my teachers who have always advised, recommended and helped me for my research work. I would not have done this research without the technical and moral support that I have received from my mentor Kanishtha Dubey. I would also like to thank the Environmental laboratory staff who have contributed to my work by being proactive to help me during my work.

Last but not the least, my deepest gratitude goes to my Father, Mr. Rajesh Vhanbatte and my mother Mrs.Jyoti Vhanbatte who have always encouraged me and supported me in my career decisions and showered me with their blessings. I thank Almighty for all the opportunities that he has endowed upon me time and again. Last but not the least I want to express my deepest gratitude to the entire organization IIT Kharagpur which has given me a chance to study at this prestigious Institute and explore my horizons as a Post graduate student.

Place: Kharagpur

Date:

Vhanbatte Shrinish

ABSTRACT

Accurate modelling of the spatiotemporal distribution of aerosol optical depth (AOD) is crucial for understanding the impact of aerosols on climate, particularly in regions like the Indian subcontinent where aerosols play a significant role in atmospheric processes. This study employs a high-resolution chemistry transport model (CHIMERE) coupled with OPTSIM (Optical properties Simulation) to simulate pre-monsoon AOD over the Indian subcontinent using a refined emission inventory. The model effectively simulates AOD with a low normalized mean error (within 40%), demonstrating its ability to capture the observed aerosol burden.

The spatial and temporal characteristics of the simulated AOD closely align with those retrieved from the Moderate Resolution Imaging Spectroradiometer (MODIS) satellite, providing validation for the model's performance. During the pre-monsoon season, elevated AOD values (> 0.5) are prevalent over the Indo-Gangetic Plain (IGP), Eastern coastline, and central India, indicating a substantial aerosol presence in these regions. Notably, the pre-monsoon AOD is consistently higher across the entire Indian subcontinent, with particularly significant enhancements (60% to 80%) over central India and the Bay of Bengal compared to other regions.

Anthropogenic aerosols dominate the contribution to pre-monsoon AOD across most of the Indian subcontinent, reflecting the substantial influence of human activities on aerosol emissions. Dust aerosols play a prominent role in northwestern India and the IGP, contributing AOD values ranging from 0.2 to 0.6. Meanwhile, anthropogenic aerosols exert a significant influence in the Eastern IGP and Eastern coastline, with AOD values ranging from 0.7 to 0.84. Interestingly, the contribution of anthropogenic aerosols is more pronounced in the Bay of Bengal compared to the Arabian Sea during the pre-monsoon season, highlighting the regional variability of aerosol sources and their impact on AOD distribution.

The findings underscore the dominance of anthropogenic aerosols in shaping AOD patterns and the significant contribution of dust aerosols in specific regions.

Contents

CHAPTER 1
INTRODUCTION

1.1 Background and Motivation

Aerosols are minute particles suspended in the atmosphere. The size of aerosol ranges from 0.002 to more than 100μm.Aerosols are ubiquitous in air and are often noticeable as dust, smoke and haze. Their scattering of sunlight can reduce visibility (haze) and redden sunrises and sunsets. Two types of environmental problems are being faced, first global climate change and second is environmental pollution. Air pollutants (mainly Ozone and aerosol particulate matter) influence Earth's radiation budget and cause climate change. Aerosol plays an important role in energy budget of the Earth, both directly by the scattering and absorption of solar-radiation and indirectly by influencing cloud information, modifying cloud lifetime, cloud condensation, nuclei formation and regulating cloud droplet number. Individual aerosol particles may contain chemically distinct species such as sulphates, organics, BC, and dust. More often they are composite mixtures of a core refractory material (BC, dust, sea salt) with a coating of organics, sulphates, and nitrates.

It is required to know the adequate aerosol optical and chemical properties of particulate atmospheric species that affects regional radiation forcing, the radiation balance, and thus climate. Since atmospheric aerosol concentrations peak close to major source regions thus giving rise to regional hot-spots, aerosol-induced radiative impact could be more significant on a local to regional scale than the global, which in turn can have strong implications for the regional hydrological cycle.

Aerosols can have both cooling and warming effects on the climate. Direct radiative forcing occurs when aerosols scatter or absorb sunlight, influencing the Earth's energy balance. For example, sulphate aerosols reflect sunlight back into space, leading to cooling, while black carbon (soot) absorbs sunlight, causing warming.

Ground-based measurements provide valuable insight into aerosol optical properties. However, the lack of a robust aerosol measurement network leads to the inconsistent spatial and temporal resolution of the measured aerosol data. The satellite measurement of aerosol optical properties is useful for consistent spatiotemporal information on aerosol but, uncertainties exist in satellite-retrieved products due to coarse resolution and several assumptions (surface reflectance, cloud screening). Atmospheric chemical transport models (CTM) help to evaluate the complex aerosol system by providing the necessary framework for integrating individual atmospheric aerosol processes and their interactions (Stier et al., 2006). Aerosol optical properties simulated in a CTM and evaluated against the measurements provide information on the fine-resolved distribution of aerosol. Furthermore, models have the provision of evaluating the specific contribution of aerosol species (e.g. dust and anthropogenic aerosol) to total AOD. Information related to the specific contribution of dust and anthropogenic aerosol is crucial for planning proper mitigation strategies related to air pollution and climate change.

The recent evaluations of aerosols with free-running CTM have shown the inadequacy of the model to simulate the spatial and temporal pattern of AOD distribution over the Indian subcontinent as indicated by satellite-based retrievals (Pan et al., 2015). In this regard, AOD at 550 nm (AOD_{550}) was found to be 2–3 times lower than the observed counterparts (MODIS AOD).

We are also able to find out that the large underestimation of aerosol concentration over the Indian mainland would primarily be due to emission data sets, instead of the model configurations. An adequate description of aerosol is necessary to assess the relative contribution of dust and anthropogenic aerosol to AOD in India (Ghosh et al., 2020). In this study, we examined the specific contribution of dust and anthropogenic aerosol to AOD over the Indian subcontinent after evaluating the efficacy of simulated aerosol optical properties in fine - resolved CTM (CHIMERE) during pre-monsoon season. It was necessary to adequately simulate the AOD and SSA in the CHIMERE model with new aerosol emissions and analyse spatial and temporal (pre-monsoon) AOD distribution alongside measurement values. It was also necessary to analyse the relative influence of emission on simulated aerosol optical properties and to estimate the AOD due to dust and AOD due to anthropogenic aerosols.

1.2 OBJECTIVES:

The specific objective of the present study are as follows:

1. Estimation of AOD (Aerosol Optical Depth) over India during the pre-monsoon period (March - April - May).

2. Validation of simulated optical properties with respect to ground-based measurements and satellite observations.

3. To estimate the contribution of anthropogenic and dust aerosols over India.

CHAPTER 2

LITERATURE REVIEW

2.1 Atmospheric Aerosols

Technically, an aerosol is defined as fine solid or liquid particle suspended in a gaseous me-dium. A wide range of phenomena are included in the aerosol category for example- dust, fume, smoke, mist, fog, haze, clouds, and smog. It is only a very small fraction of total mass and volume of aerosols, (≤ 0.0001 %) that are represented in the particulate phase (Hinds, 1999). Major percentage (89%) of aerosol emissions are from the natural sources (Moorthy et al., 2005). Among all the natural aerosol, the major contributors are soil dust and sulphate originated from ocean. Anthropogenic sources of aerosols are fuel combustion in industries, power plants and vehicles, dust from roads, wind induced soil erosion and construction sites etc. Aerosol constituents are major contributors to the airborne fine particulate matter with mass concentration of particles less than or equal to 2.5 micro meter in aerodynamic diameter (PM 2.5) (Unger, 2012). Fine particles' atmospheric lifetime varies from days to weeks and coarse particles atmospheric lifetime ranges from minutes to days. Aerosol particle affects the climate directly as well as indirectly. When aerosols directly scatter and/or absorbs the solar radiation, it is called direct effect. In the indirect effect, aerosols modify the cloud properties which in turn affect the Earth's radiation budget. Soot (i.e., black carbon) causes warming, whereas all other aerosol species causes cooling to the atmosphere. If the aerosol effects on radiation budget is effectively cooling in nature it helps in diminishing the greenhouse warming and while if the net effect of aerosol is causing warming in nature it aggravates the greenhouse warming (Smithson, 2002) . A short residence time of aerosol means that aerosols are regionally more effective and less persistent into the future than long-lived greenhouse gases. Effects of aerosol on the climate are generally defined in term of radiative forcing. It is a change in the energy fluxes

of solar radiation. The scattering of solar radiation by aerosols or clouds comes under negative forcing (i.e., cooling effects) whereas the absorption of radiation by aerosol greenhouse gases or cloud tends to warm the surface and it is called positive forcing (i.e., warming effect) (Poschl,¨ 2005). The changes in Earth's radiation budget due to scattering and absorption by aerosols are called direct radiative forcing. Aerosols also act as cloud condensation nuclei (CCN) and ice nuclei (IN) and abundance of aerosols cause increase in the number of CCN and IN . Increasing number of CCN and IN cause an increase in the number concentration of cloud droplets which in turn leads to an increase in the reflection of solar radiation from clouds resulting in climate cooling (i.e., first indirect radiative forcing). If the increase in aerosols does not alter the condensed moisture inside the cloud, the radius of cloud drop will decrease causing a de-crease in precipitation efficiency. Precipitation in polluted clouds get suppressed due to this micro-physical effect . It can also lead to high amount of clouds and can also increases clouds' lifetime. This increase in cloud lifetime means increase in the reflection of solar radiation and this effect is termed as second indirect radiative forcing.

2.2 Aerosol Species

Atmospheric aerosol particles generally comprise of nitrates, ammonium, organic material, sulphates, sea salt, crustal species, hydrogen oxides, metal oxides, hydrogen ions, and water. Among all these species sulphate, ammonium, organic and elemental carbon, and certain transition metals are found predominantly in the fine particles. Coarse fraction of aerosol are usually found in crustal materials. Nitrates can be found in both fine mode as well as coarse mode. An average chemical composition of aerosol system which is evolved for the Northern Hemisphere is composed of 30% sulphate, 25% carbon, 32% dust and 13% sea salt respectively (Chin et al., 2004).

An average chemical composition of aerosol in the wintertime evolved for a rural region (Viz., Kharagpur) in Indo Gangetic Plain (IGP) shows that the total aerosol is composed of 17% dust, 18% water-soluble components, 6% black carbon (BC), 23% particulate organic matter (POM) along with a residual fraction (i.e., organic fraction of natural or anthropogenic and

water content of aerosols) of 36% (George et al., 2011)

For Trivandrum, Kerala the chemical composition in wintertime is observed to be 29% water soluble, 51% Particulate organic matter, 11% black carbon, 8% mineral dust and 1% residual fraction (George et al., 2008). For Kanpur (as industrial city), a percentage contribution of water soluble portion is 34% to the total aerosol mass (Tare et al., 2006), contribution of BC concentration to total mass is found to vary between 7-15% (Tripathi et al., 2005) in winter-time. In Delhi, contribution of Total Carbonaceous Aerosol mass (which consists of organic carbon and black carbon or elemental carbon) to PM2.5 mass is found to be 46% for wintertime respectively (Tiwari et al., 2013).

In India, coarse mode aerosols are in abundance particularly during summer season while during winter, accumulation mode particles are found in abundance over urban environment. Aerosols are found in low concentrations during the monsoon season due to wet deposition caused by rainfalls. Fractional contribution of black carbon aerosols in total aerosol is around 15% over the year (Latha and Badarinath, 2005). Wet deposition of aerosol by precipitation is the most effective way to decrease the aerosol concentration near the surface. Increase in relative humidity during summer-monsoon causes hygroscopic growth in water-soluble aerosols leading to increased AOD. This leads to removal of water soluble aerosol and addition of sea salt in the atmosphere (Ramachandran and Kedia, 2013). The major contributor of aerosol is organic in nature with less contribution from sea salt across India (as shown in Table-2.1). Those regions which are less developed (i.e., Eastern India) generally have the highest concentration of black carbon and organic carbon

Less developed regions like the Eastern India has the highest levels of Organic Carbon (OC) and black carbon (BC). Sum of organic and black carbon (Table-2.1) concentration is closely associated with domestic activities like wood burning for cooking, trash, burning of agricultural waste products. Combined contribution of OC and BC to total aerosol loading is approximately 18–32% over many Indian regions. OC and BC are mostly found in fine mode and are mostly generated by human activities (David et al., 2018).

Table 2.1: Percentage contribution of aerosol constituents over different regions of India. BC: black carbon; OC: Organic carbon IGP: Indo-Gangetic Plain

	Aerosol components (%)				
Regions	Inorganic	BC	OC	Dust	Reference
Northern India	64	4	17	14	(David et al., 2018)
IGP	58	7	24	10	
Eastern India	60	6	26	7	
Western India	412	4	14	32	
Central India	62	5	18	12	
Southern India	62	5	17	11	

2.3 Aerosol Measurements

Aerosol measurements can be done through ground-based measurements and satellite based measurements. Under ground-based measurements, various types of instruments are used such as Sunphotometer to measure Aerosol Optical Depth (AOD), Nephelometer to measure single scattering albedo (SSA), aethalometers to measure black carbon (BC) mass. To provide an overview of ground-based sunphotometry measurements, a no. of aerosol monitoring networks including Aerosol Robotic Network (AERONET), Multi-filter Rotating Show band Radiometer (MFRSR), Maritime Aerosol Network (MAN) are used. AERONET is commonly used at global scale over land. The ground-based measurements are the simplest and the most accurate monitoring system for aerosols. Maintenance is also easy for ground-based monitoring system. Aerosol optical depth (AOD) is the most important parameter to remotely measure the atmospheric aerosol burden (Holben et al., 2001). AOD is an index of total columnar loading of aerosols in the atmosphere. AOD depends on wavelength. Global Atmosphere watch (GAW) guidelines recommend AOD be measured at three or more wavelengths among 368, 412, 500, 675, 778, 862 nm with a bandwidth of 5 nm. An AOD value of 0.01 indicates an extremely

clean atmosphere, and an AOD value of 0.4 indicates a very hazy atmospheric condition (Kusmierczyk´-Michulec, 2011).

2.4 Optical properties of Atmospheric Aerosols

Aerosols' optical properties cause many spectacular effects in the atmosphere, for example-halos around the sun or moon, rainbows, richly coloured during-sunsets. These are also cause the degradation of visibility associated with atmospheric pollution. An important class of instruments which are used for measuring aerosol concentration and its size, work on the basis of aerosol's nature of interacting with light (Hinds, 1999). The important aerosol optical properties includes Aersosl optical depth (AOD), single scattering albedo (SSA) and asymmetry parameter. AOD is function of the particle size, the complex refractive index of the particles and wavelength of the incident light (Seinfeld et al., 2004). The best parameter that quantifies the direct aerosol effect is AOD. It measures the extinction of solar radiation by aerosols scattering and absorption. It is the total reduction of incoming solar radiation while passing from TOA (i.e., top of atmosphere) to the surface. AOD indicates about the amount of direct sunlight that is prevented by aerosols to reach the ground. AOD is a dimensionless number that indicates about aerosol columnar loading over a given site. Aerosol extinction coefficient is defined as the fractional loss in Intensity of radiation per unit path. It states the attenuation of the solar radiation over a given distance travelled. The SSA value over a region explains the aerosols' scattering or absorption property. It is an important parameter to investigate the atmos

pheric heating. The scattering and absorption property of different aerosol in addition to surface reluctance helps to decide between cooling and warming effects of aerosol (Satheesh et al., 2002). The highest extinction coefficient is recorded in India during winter months (December, January, and February) while the lowest value occurs in the months September, October, and November. 75% haze exceedes in relation to distance 0.5 km^{-1} is observed annually, which corresponds to a visibility of less than 4 km. The high-elevation regions are observed to have much lower extinction coefficient which indicates that these regions are generally above the shallow haze layer that covers the Northern parts of the Indian subcontinent (Husar et al., 2000).

Table 2.2: AOD value over Indian stations at different wavelength.

Location	Time period	Wavelength (μm)	AOD	Reference
Kanpur	April-July (2004)	0.44 - 0.87	0.77 ±0.29	(Tripathi et al., 2005)
Kharagpur	December (2004)	0.38 - 0.87	0.7	(Niranjan et al., 2006)
Delhi	December (2004)	0.37 - 0.95	0.91 ±0.48	(Ganguly et al., 2006)
Bangalore	December (2004)	0.38 - 0.87	0.24	(Babu et al., 2002)

2.5 AOD Scenario over India

2.5.1 Annual trend of AOD at different stations over India Mainland

AOD shows a decreasing trend (i.e., -0.72) from 2001-2012 in semi-arid region (Babu et al., 2013) and an increasing trend (i.e., 1.97) in industrialised urban regions (Moorthy et al., 2013) of Southern part of India. Industrialized urban region has a higher AOD value than semi-arid regions of Southern India. Increasing trend of AOD (i.e., 1.56) for industrialised urban location in IGP. AOD shows Increasing trend (i.e., 1.52) over northern part of India. Central peninsula shows an AOD trend higher than that of Southern and northern parts of India. AOD shows increasing trend (i.e., 4.49) for north eastern India.

Northern India has comparatively higher AOD value than Southern India. Northern India shows high annual variability in aerosol loading due to presence of dust over Northern India particularly during summer months (i.e., March-June). As inferred from air mass trajectories and chemical composition of aerosols there are mainly three source regions of dust that has an effect over Northern India: Oman, southwest Asian basins, and Thar Desert in Rajasthan, India (Pandithurai et al., 2008).

2.5.2 Seasonal trend of AOD at different stations over the India Mainland

The Ganga basin, bounded by Himalayas in the north, extends 2000 km in East-West and about 400 km in North-South direction. Due to its generally low elevation the Ganga basin has very high level of AOD as aerosols gets accumulated over the plain (Prasad et al., 2006). Very high AOD (> 0.6) is observed in summer in basin south of Himalayan mountain range. In India, Southern parts show a much cleaner environment with AOD < 0.4 in the summer season. AOD shows higher (0.5 in the East India near Kolkata and 0.6 in north central part of India near Kanpur) during monsoon season because drought occurred in 2002 . However, Prasad et al. (2006) reported that AOD is unusually high (0.5) in the central part of the Indo-Gangetic plane (Kanpur and Vanarasi region) and the Eastern part of the Ganga basin (Kolkata) during winter season. AOD during spring season is less than 0.6 over most parts of the Indian subcontinent. Winter Monsoon AOD shows at Bengal part of the Gangetic plain in an urban (Kolkata) is slightly higher than that in semi-urban region (Kharagpur) (Kumar and Verma, 2016). AOD shows slightly higher value in winter than in summer season in Eastern India urban locations (Pani and Verma, 2014).

2.6 Aerosol retrievals using measurements of aerosol optical depth

In order to assess the climatic effect of aerosols, it become an important study to find the composition of aerosol and the source regions associated to it (Giles et al., 2012). Composition of aerosol over IGP have been studied since decade based on quantitative analysis of aero-sols' ground-based measurements (Ram et al., 2010; Sharma et al., 2007; Tare et al., 2006), and Aerosol Robotic Network (AERONET) retrievals (Arola et al., 2011; Dey et al., 2006). (Schuster et al., 2005) derived BC columnar concentration and specific absorption coefficient using refractive index data obtained from AERONET. This inversion approach helped them to get a consistent specific absorption coefficient. To get the surface BC concentration, (Dey et al., 2006) a hypothesis is developed by them on the basis of aerosol's volumetric size distribution, absorption coefficient and planetary boundary layer height. They succeeded in getting a consistent BC estimates with respect to measured value, however, this study is done for just a single location. Comparative study of model simulated and measured by AERONET for organic carbon (OC)

indicates that model is showing underestimation at urban stations and overestimation at such stations which are near biomass burning sources (Arola et al., 2011). Although under this study aerosol's chemical composition has been inferred yet there is lack of detailed information related to relative contribution of different aerosol species and the associated emission sources at a receptor site. Qualitative analysis of aerosols type division corresponds to source sectors using remote sensing techniques includes combined information on aerosol absorption and aerosol size properties (obtained from AERONET measurement data) as a part of Tigerz Intensive Operative Programme campaign (IOP) (Dumka and Kaskaoutis, 2014; Giles et al., 2012; Srivastava and Bisht, 2012).
Thus aerosol classification by most of these studies are subjective in nature. These studies are unable to provide aerosol composition, aerosol optical depth for different aerosol species and source regions associated with aerosol emission. Climate models are useful in retrieving such relevant information related to aerosol studies (Reddy et al., 2005; Verma et al., 2008, 2007)

2.7 Mathematical atmospheric transport Model

The atmosphere is an extremely complex reactive system in which numerous physical and chemical processes occur simultaneously. Ambient measurements give us only a snapshot of atmospheric conditions at a particular time and location. An understanding of individual atmospheric processes (chemistry, transport, removal, etc.) does not imply an understanding of the system as a whole. Mathematical models generally provide the necessary framework for integration of our understanding of individual atmospheric processes and study of their interactions.

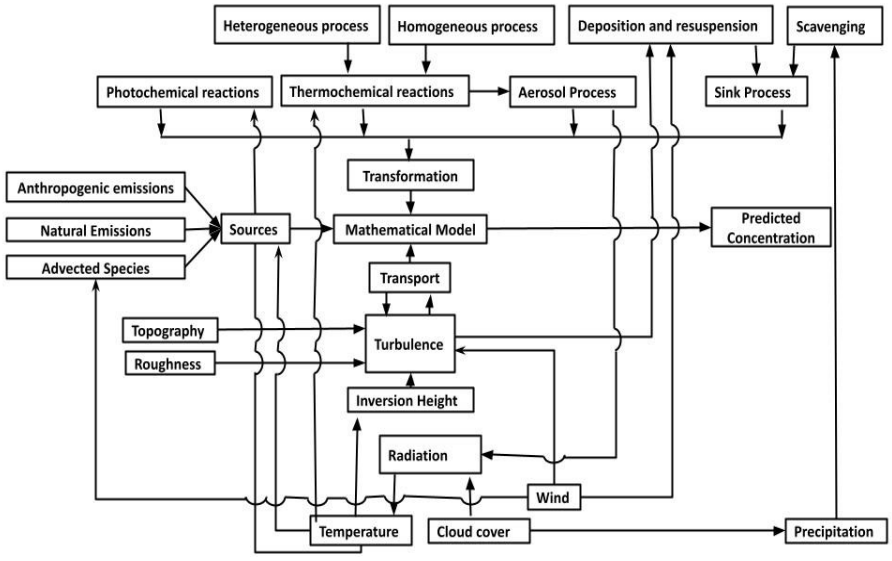

Figure 2.1: Elements of a mathematical atmospheric transport model

2.7.1 Elements of a mathematical atmospheric transport model

Basic components of Atmospheric Chemical Transport Model are- Species emissions, transport, physio-chemical transformations:

We should note the close interaction among ambient monitoring, laboratory experiments, and modelling. Monitoring (routine or intensive) identifies the state of the atmosphere and provides data needed for use and evaluation of atmospheric models. Laboratory studies generally focus on a single atmospheric process, providing parameters needed by atmospheric models. Models are the tools that integrate our understanding of atmospheric processes.

2.7.2 Types of mathematical atmospheric transport model

Mathematical atmospheric transport models, based on framework are mainly divided into Lagrangian Models and Eulerian Models. Lagrangian models simulate changes in the chemical composition of a given air parcel as it is advected in the atmosphere, while Eulerian models describe the concentrations in an array of fixed computational cells.

Based on dimensions mathematical atmospheric transport model are divided as 0-D (Box models), 1-D (column), 2-D and 3-D models. In a box model, concentrations are same every-where and therefore are the functions of time only i.e., c(t). 1-D model assumes that concentrations are functions of height and time: c_i (z, t). The modeling domain consists of horizontally homogeneous layers. 2-D models assume that species concentrations are uniform along one dimension and depend on the other two and time, for example: c_i (x, z, t). 3-D models simulate the full concentration field: c_i(x,y,z,t).

2.7.3 Numerical Solution of Chemical Transport Model (CTM)

A box model (0-Dimensional) is based on the mass conservation of a species inside a fixed Eulerian box of volume H $\Delta x \Delta y$ The box is assumed to have a height H{t) equal to the mixing-layer height. This mixing height may be allowed to vary diurnally to simulate the evolution of the atmospheric mixing state. A mass balance for the concentration c_i of species i results in model following equation.

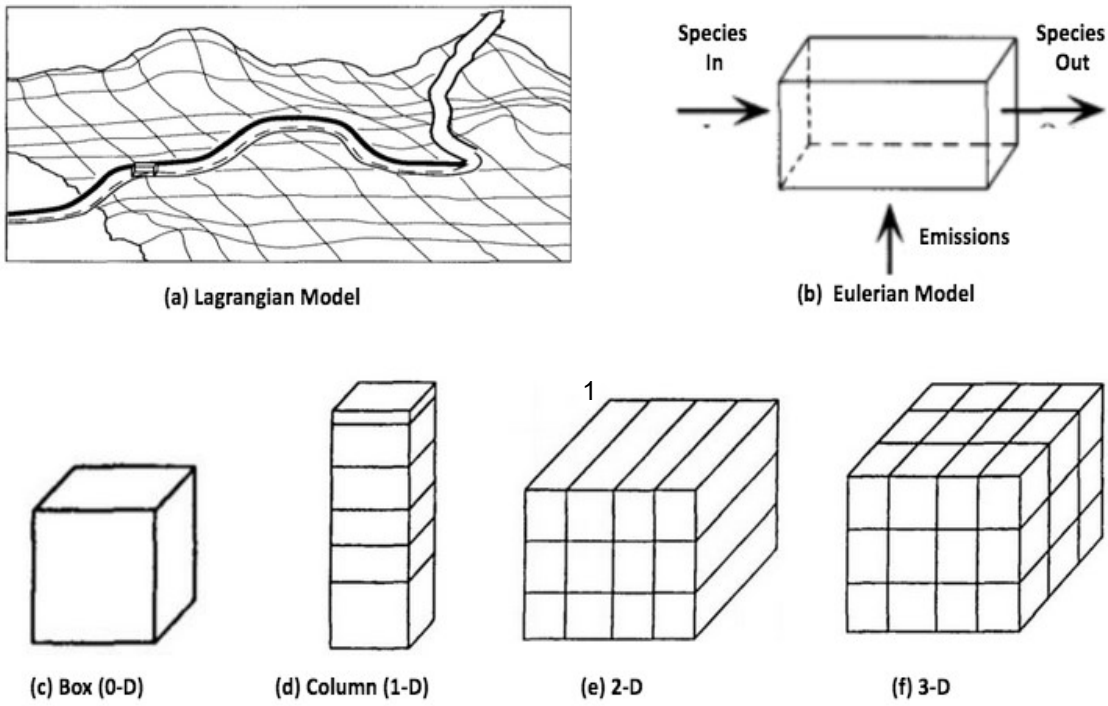

Figure 2.2: Types of a mathematical atmospheric transport Models

$$\frac{d}{dt}(c_i \triangle c \triangle y H) = Q_i + R_i \triangle x \triangle y H - S_i + uH \triangle y (c_i^0 - c_i) \qquad (2.1)$$

where:

Q_i: mass emission rate of i (Kgh^{-1});

S_i: removal rate of i (Kgh^{-1})

R_i: Chemical production rate of i ($Kgm^{-3} h^{-1}$)

c_i^0: background concentration

Simplifying mass balance equation gives the entraining Eulerian box model equations as follow.

$$\frac{d}{dt}c_i = \frac{q_i}{H(t)} + R_i - \frac{v_{d,i}}{H(t)}c_i + \frac{(c_i^0 - c_i)}{\tau_r}; \quad for \quad \frac{dH}{dt} \leq 0 \qquad (2.2)$$

$$\frac{d}{dt}c_i = \frac{q_i}{H(t)} + R_i - \frac{v_{d,i}}{H(t)}c_i + \frac{(c_i^0 - c_i)}{\tau_r} + \frac{(c_i^0 - c_i)}{H(t)}\frac{dH}{dt}; \quad for \quad \frac{dH}{dt} > 0 \qquad (2.3)$$

where: τ_r(Residence time) = $\frac{\triangle x}{u}$

The mass balance for the Lagrangian box is identical to Eulerian box model with the exception that the advection terms are absent:

Mass balance equation for three dimensional atmospheric chemical transport models is as follow.

$$\frac{dc_i}{dt} = \nabla.(uci) = R_i(c_1, c_2 \ldots\ldots\ldots c_n) + E_i - S_i \qquad (2.4)$$

where:

$c_i(x, t)$: concentration of i as a function of location x and time t

$u(x, t)$: velocity vector (u_x, u_y, u_z)

R_i: chemical generation term for i

$E_i(x, t)$: emission fluxes

$S_i(x, t)$: removal fluxes

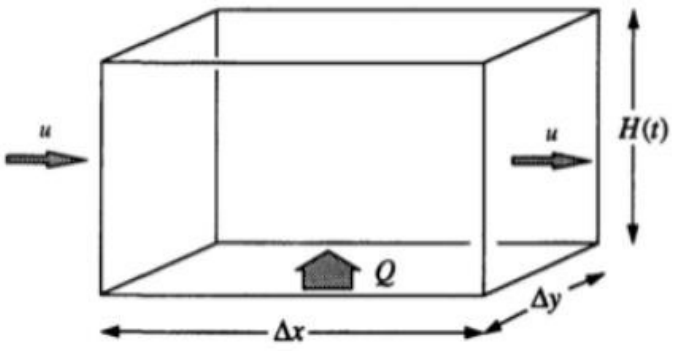

Three dimensional Chemical transport models solve chemical species equations of the general form.

$$\frac{\partial Ci}{\partial t} = \frac{\partial Ci}{\partial t}adv + \frac{\partial Ci}{\partial t}diff + \frac{\partial Ci}{\partial t}cloud + \frac{\partial Ci}{\partial t}dry + \frac{\partial Ci}{\partial t}aeros + R_{gi} + E_i \quad (2.5)$$

RHS terms represent the rate of change of C_i due to advection, diffusion, cloud process (wet deposition, cloud scavenging, aqueous phase reaction), dry deposition, aerosol processes (transport between gas and aerosol phases, aerosol dynamics), net production from gas phase reaction and emission rate respectively. Each phenomena on RHS is distinctly different in basic character, each usually requiring quite different numerical techniques to obtain numerical solutions. Several methods have been proposed for their solution including global finite differences, operator splitting, finite element methods, spectral methods, and the method of lines. Operator splitting, also called the fractional step method or time-step splitting, allows significant flexibility and is used in most atmospheric chemical transport models.

Operator Splitting

Operator splitting is the most popular technique for the solution of chemical species equations of the general form. Instead of solving the full equation at once, we solve independently the pieces of the problem corresponding to the various processes and then couple the various changes resulting from the separate partial calculations. If each one-dimensional method is stable, then the overall splitting technique is usually stable. Operator splitting methods require less computational resources but demand more thought. In general, stability is not guaranteed. However, operator splitting allows the use of the best available numerical technique for each modulqe.

2.7.4 Diffusion operator

Diffusion operator solves following differential equation.

$$\frac{\partial c}{\partial t} = \frac{\partial(k_{xx} * \frac{\partial c}{\partial x})}{\partial x} + \frac{\partial(k_{yy} * \frac{\partial c}{\partial y})}{\partial y} + \frac{\partial(k_{zz} * \frac{\partial c}{\partial z})}{\partial z} \quad (2.6)$$

Because of its physical nature diffusion tends to smoother out the gradient and land overall

stability into physical processes. Most typical finite difference or finite element procedures are quite adequate for solving diffusion type operator problems.

Explicit scheme of finite difference method can not be used efficiently because stability condition dictates requirement for a smaller time step. Thus implicit schemes of finite difference methods are used by diffusion operators. Implicit algorithms that can be used include globally implicit algorithm such as the Crank Nicholson algorithm.

Chemical Kinetics

Gas-phase chemistry operator involves solution of system of ordinary differential equation of following form.

$$\frac{dc_i}{dt} = P_i - c_i * L_i \qquad (2.7)$$

Where:

c_i: are species concentrations

P_i= production term

$c_i * L_i$=loss term

Above equation is a system of coupled non linear differential equation. The P_i, L_i terms are functions of concentrations c_i and provide the coupling among the equations. The simplest method for solution of such equation is based on finite difference approach similar to one used by diffusion operator.

Advection Operator

Advection operator solves following partial differential equation.

$$\frac{\partial c}{\partial t} + U_x\left(\frac{\partial c}{\partial x}\right) + U_y\left(\frac{\partial c}{\partial y}\right) + U_z\left(\frac{\partial c}{\partial z}\right) = 0 \qquad (2.8)$$

Finite difference method for advection operator gives a numerical error, known as numerical diffusion (solution ”diffuses” artificially into the next grid cell). Different schemes (Upwind,

Vanleer) are used in different models to solve the advection operator without this numerical diffusion.

In the upwind scheme , the fluxes at the cell interfaces are defined by the following equations according to the sign of the wind speed at the cell interface. In this scheme it is assumed that the tracer concentration is uniform in each grid cell. The mass flux at the interface is the product of the wind speed at the interface and tracer concentration in the upwind cell. Van leer scheme assumes that the concentration inside a grid cell is described by a linear slope between the two cell interfaces. This scheme is recognised in meteorology for its numerical accuracy and smaller diffusion than the upwind scheme but slightly more time-consuming than the upwind scheme. In meteorology, it can be considered as a good compromise solution between numerical accuracy and computational efficiency for long-range transport.

The piecewise parabolic method (PPM) scheme is a 3rd order scheme, with slope-limiting and monotonicity-preserving conditions. This scheme is applied for each dimension separately, which formally limits the model to 2nd order accuracy in solving the two-dimensional transport problem because the cross derivative $\partial^2 C/\partial x \partial y$ is not taken into account. Since the scheme is symmetric, it can be considered that the errors due the neglect of cross-derivatives approximately compensate. since the treatment of transport in each horizontal dimension has 3rd order accuracy, the PPM scheme as implemented in CHIMERE is much less diffusive than the simple 2^{nd} order Van Leer scheme.

Comparison between the three available transport schemes suggests that choice of one or another of these transport schemes has a strong impact on modelled dust concentrations. Simulated peak values of the dust plume are reduced by 32 % (upwind) or 17% (Van Leer) compared to the less diffusive PPM scheme. The plume area, defined as the surface around the peak where dust concentration exceeds 40 % of the peak value, is increased by 48 % (upwind) or 25 % (Van Leer) compared to the PPM scheme. Horizontal transport schemes also have an indirect im-pact on vertical transport and diffusion, and the most diffusive horizontal schemes tending to increase dust transport towards the lowest layers, increasing their domain-averaged surface concentrations and decreasing domain-averaged concentrations in and above the boundary layer.

CHAPTER 3

METHODOLOGY

3.1 Experimental setup for simulating spatial distribution of aerosol optical properties over India

The flow diagram for the simulation of aerosol optical properties (AOD and SSA) over India is shown in Figure 3.1. High-resolution ($0.25^{o}\times0.25^{o}$) aerosol transport simulations are carried out with a state-of-the-art Eulerian chemical transport model (CTM), CHIMERE (Described in Section 2.3). CHIMERE model is also provided with emission fluxes externally and initial and boundary conditions from the global model Laboratoire de Met`eorologie´ Dynamique General Circulation Model coupled with Interaction with Chemistry and Aerosols (LMDZ4 INCA3). Simulated aerosol concentrations are utilized by OPTSIM (please refer to Section 3.3) to calculate aerosol optical properties(total and fine mode aerosol optical depth (AOD), single scattering albedo.) at given wavelengths. A detailed information about OPTSIM is given in Section 2.6. Simulations are carried out over the domain spanning from 6^{o}N to 38^{o}N and 68^{o}E to 99.25^{o}E including the IGP region. Twenty vertical sigma pressure levels ranging from 997 to 130 hPa are considered in the present study. While aerosols and precursors are released up to different altitudes starting from the surface, depending on the source type, during pre-monsoon. Emissions from fossil fuel combustion at large point sources (LPS), usually using tall stacks, are released in the model layers 3 to 5 (height ranging from 110 m to 275 m). Large-scale open biomass burning emissions are known to be released at higher altitudes due to thermal buoyancy and are therefore emitted in the model layers 6 to 10 (heights ranging from 400 to 1800 m) (Reddy et al., 2005). Aerosol transport simulations are performed for the winter (November-February) and pre-monsoon (April-May) seasons of 2015, keeping a spin-up time of 30 days. We have validated the model's outputs with available ground-based and satellite observations.

Table 3.1: Experimental setup for simulating aerosol optical properties using recently available emission inventories.

Experiment	Emission database	Aerosol species	Region of database (Resolution)	References
Smogsimu	Smog-India	(BC, OC, SO_2, NO_x, NH_3, OPM_{25})	Indian, bottom-up ($0.25^\circ \times 0.25^\circ$)	(Pandey et al., 2014; Sadavarte and Venkataraman, 2014)
Constrsimu	Constrained EDGAR	(BC, OC, SO_2, IOM) (NO_x, NH_3)	Indian ($0.25^\circ \times 0.25^\circ$) Global, bottom-up ($0.1^\circ \times 0.1^\circ$)	Verma et al. (2017) (Janssens-Maenhout et al.)

Table 3.2: Aerosol module in CHIMERE

Details of the aerosol module of CHIMERE	
Number of bins	10 (Mass-median diameter interval: 0.039, 0.078, 0.156, 0.312, 0.625, 1.25, 2.5, 5, 10, 20, 40 μm)
Aerosol mixing	Internal homogeneous
Aerosol dynamics	Absorption, nucleation, coagulation, aging of aerosol
Deposition	Dry deposition and in the cloud or below cloud wet deposition

3.1.1 Chemical transport model, CHIMERE

CHIMERE is a regional chemical transport model designed to model ten gaseous species and aerosols. For chemistry, the gaseous mechanism MELCHIOR2 is used (Derognat et al., 2003). The estimation of aerosols is as described in (Bessagnet et al., 2004) with ten bins, with a mean mass median distribution ranging from 0.039 to 40 μm and for primary particulate matter [i.e., black carbon (BC), organic carbon (OC), and PPM the remaining part of primary emissions], sulphate, nitrate, ammonium, sea salt, and water. Secondary organic aerosols are formed following (Bessagnet et al., 2004). Chemical concentration fields are calculated with a time-step of a few minutes (using an adaptive time-step sensitive to the mean wind speed). For radiation and photolysis, the online FastJX model is used (Wild et al., 2000). CHIMERE assumes internal homogeneous mixing of aerosol it means the different chemical species are assumed to be well mixed in each size bin. The horizontal transport is calculated with the VanLeer scheme (van Leer, 1979) and vertical using an upwind scheme with mass conservation (Menut et al., 2013). Additional information about CHIMERE model is provided in Table-3.2 Boundary layer height is diagnosed using the Troen and Mahrt (1986) scheme, and deep convection fluxes are calculated using the Tiedtke (1989) scheme. Gaseous and aerosol species can be dry or wet deposited, and fluxes are computed using the Wesely (1989); (Zhang et al., 2001) parameterization. Initial and boundary conditions are estimated using global model monthly climatology calculated with the Laboratoire de Met´eorologie´ Dynamique General Circulation Model coupled with Interaction with Chemistry and Aerosols (LMDz-INCA) (Szopa et al., 2009).

3.2 Emission inventories

In the present study, two simulations are carried out subjected to the same model processes with CHIMERE but both are implementing different aerosol emission inventories. The aerosol emission inventories include recently estimated India-based– (i) Bottom-up emissions (Smog-India)

and (ii) Constrained. Spatially and temporally resolved constrained aerosol emission over India is taken as per Verma et al. (2017). The observationally-constrained aerosol emissions were estimated over the Indian region constraining the simulated aerosol concentration in a general circulation model (i.e., Laboratoire de Met´eorologie´ Dynamique atmospheric General Circu-lation Model (LMDZT-GCM)) with the observed aerosols by combining forward and receptor modelling approaches (Kumar et al., 2018; Verma et al., 2017). In the present study the aerosol transport simulation in CHIMERE corresponding to emission database- Smog-India and Constrained are referred to as, respectively, Constrsimu and Smogsimu.

3.3 Simulation of aerosol optical properties in OPTSIM

OPTSIM is a post-processing tool, designed for a complete comparison of aerosol concentration distributions calculated by chemical transport models (CTM) to passive and active remote-sensing observations (Stromatas et al., 2012). OPTSIM is developed for such CTM in which the aerosol size distribution is represented by size sections (i.e., bins). Each bin corresponds to a specific diameter range while the cut-off diameters are provided for each bin. This can be modified according to the model configuration. In OPTSIM the aerosols size distribution is interpolated to a finer resolution to ensure the best integration as far as possible where the aerosol concentration number is optically active. Simulating the aerosol optical properties (AOD, SSA) it allows an evaluation of the horizontal and temporal distributions of aerosol compared to passive remote-sensing observations. Optical properties are estimated using the 3-dimensional aerosol mass concentration obtained from a CTM like CHIMERE. In Internal homogeneous mixing of aerosols, the different chemical species are assumed to be well mixed in each size bin. To reflect the chemical and optical average of the aerosol population a volume-weighted complex refractive index is calculated from the refractive index of pure species. Non-sphericity of particles such as mineral dust is theoretically and experimentally identified as a source of bias in simulated aerosol optical properties (Dubovik et al., 2002b) and should be considered cautiously when interpreting the results. The complex refractive indices and density values are taken from the ADIENT/APPRAISE technical report (http://www.met.reading.ac.uk/adient/)

3.4 Description of observational data for model evaluation

We have used satellite and ground-based observations to compare with our simulated values. These included AERONET data for the stations shown in Figure 4.7 and MODIS satellite observations. For this study, we used AOD measurements from MODIS instruments aboard the Terra satellites. Terra satellites cross the equator, respectively, at ~10:30 a.m. (Local Time). We used the Level 3 collection five retrieval MODIS aerosol product. The AOD obtained from the satellite estimates exhibits gaps over specific grid cells (over deserts, coincident with clouds and snow-covered areas). To fill the grids with missing values, we have merged AOD from MODIS and AOD from freesimu of the GCM-indemiss in the following way to obtain constrained AOD for empty grid shells. A detailed explanation on constrained AOD can be found in Bharat et. al, 2018:

if,

4. $^{o}(i, j, t) > \tau^{m}(i, j, t)$ (which is always the case with GCM-indemiss)

then,

$$\tau^{c}(i, j, t) = \tau^{o}(i, j, t) \tag{3.1}$$

and if,

$\tau^{o}(i, j, t)$ is undefined over grid box (i, j) of MODIS data,

then

$$\tau^{c}(i, j, t) = \tau^{m}(i, j, t) \times \overline{s_f(t)} \tag{3.2}$$

where s_f is a scaling factor that is obtained as the ratio of the average values of τ^{o} and τ^{m} sampled over grid boxes with available MODIS data over the study region. The spatial distribution of winter and pre-monsoon mean of τ^{c} obtained using MODIS data is shown in Figure 4.6a and Figure 4.6d respectively.

Aerosol Robotic Network (AERONET) is a ground-based Sun/sky radiometer that measures direct solar and diffuse sky radiance in the spectral range of 0.34e1.02 mm (Holben et al., 2001). The instrument's field of view is about 1.2 and it makes direct solar radiation measurements every 15 min.

For direct solar measurement, triplet observations are made at each wavelength for calibration (using the Langley technique) and to screen clouds. Details about the measurement protocol for AERONET, calibration techniques, methodology, data processing, and quality can be found in the literature (Holben et al., 2001; Dubovik et al., 2000). AODs derived using direct solar measurements made at Ground based observations used in this study are summarized in Table-3.3. The uncertainty in AODs calculated using the direct solar radiation measurements is less than ±0.01 for wavelength 440 nm and is less than ±0.02 for shorter wavelengths (Dubovik et al., 2000).

Bias in simulated estimates ($X^{modelled}$) from experiments at stations mentioned below for seasonal monthly mean is estimated with respect to observed data (X^{obs}) with the equation as follows,

$$Bias = \frac{(X_{modelled} - X_{obs})}{X_{obs}} \times 100\% \quad (3.3)$$

Where, X = AOD, SSA, RH, wind speed, and PBLH.

Statistical analysis is carried out corresponding to seasonal monthly mean to evaluate the normalised mean error (NME, Equation 3.2) and root means square error (RMSE, equation 3.3) from the simulated results for 20 stations.

$$NME = \frac{\sum_{1}^{N} X_{modelled} - X_{obs}}{\sum_{1}^{N} X_{obs}} * 100\% \quad (3.4)$$

$$RMSE = \left[\frac{1}{N}\sum_{1}^{N} (X_{modelled} - X_{obs})^2\right]^{\frac{1}{2}} \quad (3.5)$$

Where, X = AOD, SSA, RH, wind speed and PBLH

3.5 Data assimilation

Data assimilation is the technique by which observations are combined with an NWP product (the first guess or background forecast) and their respective error statistics to provide an improved estimate (the analysis) of the atmospheric (or oceanic, Jovian, etc.) state. Variational (Var) data assimilation achieves this through the iterative minimization of a prescribed cost (or penalty) function. Differences between the analysis and observations/first guess are penalized (damped) according to their perceived error. The difference between three-dimensional (3D-Var) and four-dimensional (4D-Var) data assimilation is the use of a numerical forecast model in the latter.

Table 3.3: Data from measurements at available locations used to validate the estimated results over India

Type of Region	Station	Location	Data (Year of) Measurement)	Reference(s)
Megacity	New Delhi (NDL)	28.70°N, 77.10°E	AOD (2008-09) SSA (2010) PBLH (2006)	Soni et al. (2010); AERONET Ramachandran et al.,(2015) Bano et al. (2011)
	Kolkata (KOL)	22.57°N, 88.36°E	AOD (2009-11) SSA (2009-10)	Kumar et al. (2018) Pani and Verma., (2014)
	Mumbai (MUB)	19.13°N, 72.91°E	PBLH (2015)	Kedia et al. (2018)
	Chennai (CHN)	13.08°N, 80.27°E	AOD (2013)	Aruna et al. (2016)
Urban	Kanpur (KNP)	26.51°N, 80.23°E	AOD (2004-05, 2010) SSA (2010)	Nair et al. (2007); AERONET Ramachandran et al.,(2015)
	Ahmedabad (AHM)	23.02°N, 72.57°E	AOD (2008)	Ramachnandran and Kedia (2010)
	Varanasi (VRS)	25.32°N, 82.97°E	AOD (2009-10)	Singh et al. (2015)
	Visakhapatnam (VSK)	17.69°N, 83.22°E	AOD (2005-06, 2008)	Sreekanth et al. (2007); AERONET
	Trivandrum (TVM)	8.5°N, 76.94°E	AOD (2000-03)	Moorrthy et al. (2000-03)
	PUNE	18.5°N, 73.85°E	AOD (2005, 2010)	Dani et al. (2012); AERONET
	Nagpur (NGP)	21.15.10°N, 79.09°E	AOD (2008-09)	Kannemadugu et al. (2014)
	Agra (AGR)	27.10°N, 78.00°E	AOD (2004)	Safai et al. (2008)
	Jaipur (JPR)	26.91°N, 75.80°E	AOD (2010)	AERONET
Semi-urban	Kharagpur (KGP)	22.35°N, 87.23°E	PBLH (2004) AOD (2011-12, 2009) PBLH (2010)	Nair et al. (2007) Kumar et al. (2018); AERONET Nair et al.,(2007)
	Ranchi (RNC)	23.50°N, 85.30°E	PBLH (2011) AOD (2011-12)	Chandra et al. (2014) Latha et al. (2014)
	Gurugram (GRG)	28.32°N, 76.92°E	AOD (2017)	AERONET
	Bhola (BHL)	22.22°N, 90.36°E	AOD (2013)	AERONET
	Dhaka University (DHK)	23.73°N, 90.4°E	AOD (2013)	AERONET
	Karunya University (KRN)	10.93°N, 76.74°E	AOD (2014)	AERONET
	Agartala (ATL)	23.83°N, 91.28°E	AOD (2010-14)	Pathak et al. (2016)
	Anantpur (ANT)	14.68°N, 77.6°E	AOD (2008)	Reddy et al. (2010)
	Pantnagar (PTN)	29.25°N, 79.75°E	AOD (2009) SSA (2011-12)	AERONET Dumka et al., (2014)
	Dibrugarh (DBR)	23.70°N, 94.60°E	AOD (2010)	Pathak et al. (2010)
	Patiala (PTL)	30.34°N, 78.23°E	SSA (2011-12)	Singh et al., 2016
	Mahabaleshwar (MBL)	17.93°N, 73.65°E	PBLH (2011-12)	Chandra et al. (2014)
Less polluted	Darjeeling (DJL)	27.00°N, 88.27°E	AOD (2008)	Sarkar et al. (2015)
	Hyderabad (HYD)	17.38°N, 78.48°E	AOD (2009-10) SSA (2008-09)	Dumka et al. (2013) Sinha et al. (2013
	Minicoy (MNC)	8.27°N, 73.05°E	AOD(2008)	Vinoj et al. (2010)
	Nainital (NTL)	29.39°N, 79.45°E	SSA (2005-08) PBLH (2011)	Ram et al., (2010) Singh et al. (2016)
	Manorapeak (MNP)	29.22°N, 79.27°E	AOD(2005-06)	Ram and Sarin (2010)
	Dehradun (DHD)	30.32°N, 78.03°E	AOD (2007)	Singh et al. (2012)
	MCO-Hanimadho (MCO)	6.78°N, 73.18°E	AOD(2009)	AERONET

CHAPTER 4

RESULTS AND DISCUSSION

4.1 Pre-monsoon AOD variation over India

Seasonal mean of AOD_{550} simulated using constrained (AOD_{550}^{constr}) and smog (AOD_{550}^{smog}) emissions along with percentage seasonal change for both the cases is presented. Distinct spatial features of high AOD are seen over the North-Western India (NWI), Indo-Gangetic Plain (IGP), North-Eastern India (NEI) and South-Central India (SCI) during pre-monsoon season for both AOD_{550}^{constr} and AOD_{550}^{smog}. However, over the IGP, NEI and SCI regions, AOD_{550}^{constr} is higher (~2-3 times) than AOD_{550}^{smog}. During the winter sea-son, AOD_{550}^{constr} is higher than AOD_{550}^{smog} over most parts of India, although the spatial features are similar for both the cases with the highest AOD_{550} being seen over the lower IGP region.

An increase in the seasonal AOD_{550} is seen for both AOD_{550}^{constr} and AOD_{550}^{smog} during pre-monsoon as compared to winter (Figure 4.4). However, the seasonal increase in AOD_{550}^{smog} is higher than AOD_{550}^{constr} with distinctive regions with very high percentage (70%-90%) increase over northwestern India. Seasonal increase in AOD_{550}^{smog} during pre-monsoon with respect to winter is in a range of 30-60% over most parts of India (Figure 4.4 f). A relatively lower change in AOD_{550}^{smog} (i.e., 5-25% increase) is noticed over the Southern parts of both the Bay of Bengal (BOB) and the Arabian Sea (AS). Region specific drastic seasonal increasing feature (as high as 95% increase) in AOD_{550}^{smog} is seen over the NWI region, the second highest being over the central and South India (CSI, 60-75% seasonal increase)

Overall seasonal increase in AOD_{550}^{constr} is lower than in the case of AOD_{550}^{smog} over most parts of NWI and upper IGP (ranging between 40% to 60% increase) [Figure 4.4 c]. The specific spatial features of a high percentage increase over SCI during winter is seen for AOD_{550}^{constr} also. Seasonal increase in AOD_{550}^{constr} is 2-3 times higher (lower) than AOD_{550}^{smog} over the Southern parts of the BOB

4.2 Comparison of Simulated optical properties with Observations

4.2.1 Comparison of Simulated AOD with Satellite observations

The seasonal mean of AOD at 550 nm obtained from simulations (Smogsimu and Constrsimu) is compared with that of satellite observations (MODIS) (Figure 4.6) for pre-monsoon (PMN) seasons. The higher AOD_{550}^{constr} values than AOD_{550}^{MODIS} are observed over East Central and Southern India. However this overestimation is attributed to the low observed AOD_{550}^{MODIS} in these regions. During the PMN season, the spatial pattern of AOD_{550}^{constr} showing high (> 0.5) value over the IGP and Eastern coastal regions is consistent with the features of observed AOD_{550}^{MODIS}.

The highest AOD is observed over the lower IGP region for both AOD_{550}^{constr} and AOD_{550}^{MODIS}. However, this spatial feature of high AOD over IGP is not seen in AOD_{550}^{smog}.

Table 4.1: Comparison of MODIS based AOD with Ground-Based AOD Measurement for pre-monsoon

Station	MODIS AOD	AERONET based AOD	Constrsimu based AOD
Vishakhapatanam	0.43	0.86	0.96
Kolkata	0.5	0.7	0.8
Dibrugarh	0.42	0.64	0.66

The estimated AOD_{550}^{smog} is lower in magnitude by 20%-40% than AOD_{550}^{MODIS} over most of India. The underestimation is as high as 60% over parts of IGP and Southern India. Interestingly, high AOD_{550}^{constr} (0.7–0.9) over Eastern Central and Southern India (CSI) is not at all reflected in AOD_{550}^{MODIS}. We further verified AOD in these regions with the ground-based measurement of AOD_{550} from the AERONET and found that simulated AOD values are coming closer to $AOD_{550}^{AERONET}$ than AOD_{550}^{MODIS}.

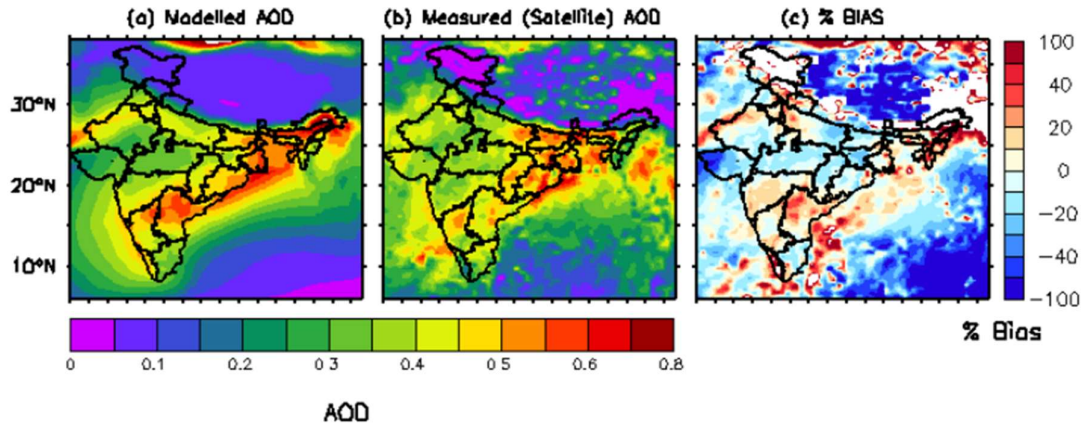

4.2.2 Comparison of Simulated AOD with Ground-based Measurements

The simulated AOD from Smogsimu and Constrsimu is compared with AERONET observations at 500 nm for pre-monsoon seasons. The AOD_{550}^{constr} matches consistently well during pre-monsoon (NME ≤ 20%) seasons. AOD_{550}^{constr} and AOD_{550}^{smog} show underestimations at all the stations except AOD_{550}^{constr} at Pune, New Delhi and Kolkata during pre-monsoon where overestimation is observed. Higher underestimation values are observed for AOD_{550}^{smog} than AOD_{550}^{constr} during pre-monsoon seasons. A comparatively higher estimated value of the normalized mean error (65%) in the case of bottom-up emission (SMOG-India) indicates that CHIMERE model could simulate the AOD over India more efficiently with constrained emission than with SMOG-India emission.

4.3 Contribution of dust and anthropogenic aerosol to AOD over India

The influence of anthropogenic aerosols (particularly absorbing aerosols) on tropical precipit-ation has become evident in recent years. Studies using different general circulation models (GCMs) indicate that direct radiative forcing (DRF) of absorbing black carbon (BC) aerosols can lead to a northward shift of precipitation in the Intertropical Convergence Zone (ITCZ) over the Pacific Ocean (Wang, 2004; Roberts and Jones, 2004; Chung and Seinfeld, 2005). Recent modeling studies also suggest that DRF of aerosols could have a significant impact on critical tropical precipitation system, the Indian summer monsoon (Lau et al., 2008). A considerable fraction of the world's population lives in the South Asian region, where much of the agricultural activity and water resources are dependent on the summer monsoon evolution. A better understanding of AOD due to anthropogenic aerosol has significant importance. In this study spatial distribution of AOD due to dust (AOD_{dust}) and AOD due to anthropogenic aerosol.

AOD_{anthro} value is found to be higher (2–3 times) over the Eastern IGP than the rest of India during pre-monsoon seasons, while over the Eastern coastal regions, western coastal regions, and Southern India, it is higher (2–3 times), particularly during pre-monsoon season. During pre-monsoon, dust AOD (0.1–0.3) was also seen over the upper IGP and central India.

The rest of the India is dominated by anthropogenic contributions. Over western India, during pre-monsoon, about 50% – 70% of total AOD comes from dust compared to that being 30% to

60% during winter. Most parts of central India are having 60% – 80% of total AOD from anthropogenic emissions during winter as well as pre-monsoon season. Over the Eastern IGP, Eastern coastal regions, and Southern India, the contribution of anthropogenic aerosol is higher during pre-monsoon (80% – 95%).

4.4 Aerosol Optical Depth (AOD) under different simulation set-ups

4.4.1 Free run AOD simulation using SMOG-India emission

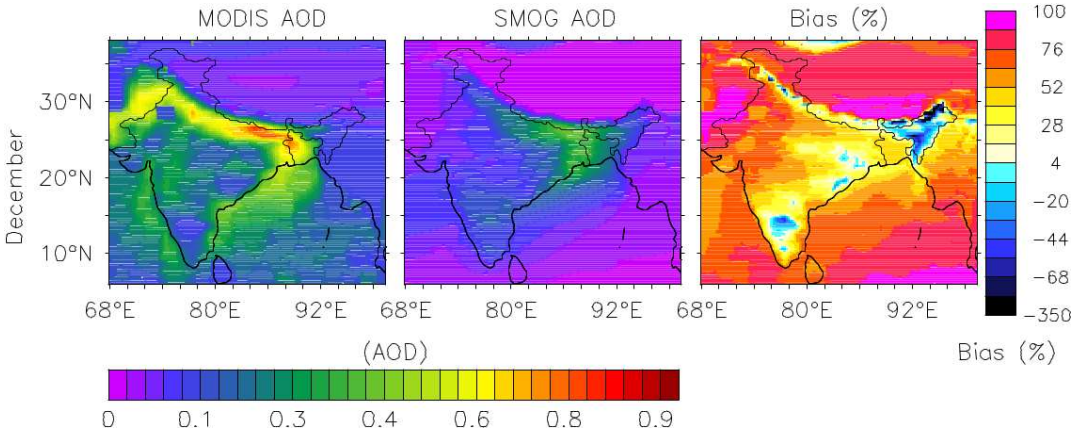

Figure 4.2: Spatial distribution of (a-b) AOD from (a) satellite observation MODIS (b) CHI-MERE using SMOG-India emission, (c) percentage bias between a and b.

In this experiment, AOD was simulated using SMOG-India emission in CHIMERE (OPTSIM) for December month. Spatial distribution of simulated AOD, observed AOD (MODIS) and percentage bias are shown in Figure 4.13. Simulated AOD is showing underestimation (2-3 times) over the entire India except over the North Eastern states and some parts of Southern India where overestimation (20%-40%) is observed. Bias between simulated and observed AOD is as high as 90% over North Western India followed by most parts of Lower IGP, East central India, and Southern India having bias varying between 25% to 50%. The spatial feature showing the highest AOD over lower IGP, as seen in MODIS AOD, is being captured by simulated AOD. Very high bias between simulated and observed AOD indicated towards a need for further experiments in order to simulate the AOD with less bias.

CHAPTER 5

SUMMARY AND CONCLUSION

Aerosols affect the Earth's climate directly by altering the Earth's energy budget through absorbing and scattering solar radiation (direct effect) and indirectly by altering the properties of clouds (indirect effects) (Boucher et al., 2013). Estimation of aerosol-induced radiative effects and their impact on climate requires accurate analysis of aerosol optical properties (aerosol optical depth (AOD), aerosol single scattering albedo (SSA), asymmetry parameter). Large variability of aerosol in space and time due to their low atmospheric lifetime, wide variety in their sizes and chemical composition lead to complexity in an accurate assessment of aerosol optical properties.

Ground-based measurements provide valuable insight into the aerosol optical properties. However, the lack of a robust aerosol measurement network leads to the inconsistent spatial and temporal resolution of the measured aerosol data. The satellite measurement of aerosol optical properties is useful for consistent Spatio-temporal information on aerosol but, uncertainties exist in satellite-retrieved products due to coarse resolution and several assumptions (surface reflectance, cloud screening). Atmospheric chemical transport models (CTM) help to evaluate the complex aerosol system by providing the necessary framework for integrating individual atmospheric aerosol processes and their interactions (Stier et al., 2006). Aerosol optical properties simulated in a CTM and evaluated against the measurements provide information on the fine-resolved distribution of aerosol. Furthermore, models have the provision of evaluating the specific contribution of aerosol species (e.g. dust and anthropogenic aerosol) to total AOD. Information related to the specific contribution of dust and anthropogenic aerosol is crucial for planning proper mitigation strategies related to air pollution and climate change.

In this study, we examined the specific contribution of dust and anthropogenic aerosol to AOD over the Indian subcontinent after evaluating the efficacy of simulated aerosol optical properties in fine-resolved CTM (CHIMERE) during pre-monsoon seasons.

It was also necessary to analyze the relative influence of emission on simulated aerosol optical properties and to estimate the AOD due to dust and AOD due to anthropogenic aerosols.

Fine-resolved aerosol transport simulations were carried out with a state-of-the-art Eulerian chemical transport model, CHIMERE, over the Indian domain spanning from 6^{o}N to 38^{o}N and 68^{o}E to 99.25^{o}E. The CHIMERE configuration (model version 2017) was used in the present study.

The second focus of this work was to carry out a detailed comparison between estimates of aerosol optical properties from simulation and observation (ground-based measurements and satellite observations). Observed AOD and SSA were retrieved for the study regions and anomalies between simulated and observed values were estimated in terms of bias (%). Bias (%) has been calculated as a percentage decrease (negative bias) or increase (positive bias) in simulated value to the observed value. To further investigate the reasons behind the bias between simulated and observed values, species-wise AODs were compared with available previous studies

The third focus of this work was to analyze the relative influences of emission inventory on the simulated aerosol optical properties and its bias to observations. For this purpose, a comparative analysis of AOD and SSA distributions from bottom-up emission (Smog-India) and constrained emission were done alongside the observation.

In the present study, we used recently available information on aerosol emission over India in a finely resolved simulation framework (WRF-CHIMERE-OPTSIM) to estimate the relative influence of emission on simulated aerosol optical properties (AOD and SSA), Spatio-temporal variation in AOD, and contribution of dust and anthropogenic aerosol to total AOD over India during pre-monsoon.

Highlights of the results are enlisted below.

1. A seasonal increase in AOD during the pre-monsoon season was observed for the modeled AOD_{550}^{constr} which was consistent with the MODIS AOD (AOD_{550}^{MODIS}). The spatial feature of high AOD_{550}^{constr} was seen similar to AOD_{550}^{MODIS} over the IGP region during pre-monsoon. During the pre-monsoon season, the spatial pattern of AOD_{550}^{constr} showing high value over the IGP, Eastern coastal regions (AOD:0.6-0.9) were consistent with the features

of observed AOD_{550}^{MODIS}. Interestingly, high AOD_{550}^{constr} (>0.7) over the Eastern central and Southern India was not at all reflected in AOD_{550}^{MODIS}. However, when we further verified AOD in these regions with the ground-based measurement (AERONET), simulated AOD values were found to be closer to $AOD_{500}^{AERONET}$ than AOD_{550}^{MODIS}. The AOD_{550}^{constr} matched consistently well with AERONET AOD during both winter (NME ≤ 25%) and pre-monsoon (NME ≤ 5%) seasons. AOD_{550}^{constr} showed underestimations at all the stations except Kolkata and Pantnagar, where overestimation was observed. The monthly mean measured SSA at 500 nm was well simulated by the model with low bias (< 10%), thus indicating the modelled SSA being consistent with measurements.

2. During the pre-monsoon season, the estimated AOD_{550}^{smog} was lower in magnitude by 10%-40% than AOD_{550}^{MODIS} over most of India. The underestimation value was comparatively higher over parts of IGP and Southern India.

3. Dust AOD during winter was very low (i.e., < 0.1) over the entire India, while during pre-monsoon, it was high (0.3–0.6) over western India. During pre-monsoon, dust AOD was also seen over upper IGP and central India. Over western India during pre-monsoon, about 30% to 70% of total AOD was from dust compared to that being 30% to 60% during winter. Over the rest of India, 60% to 90% of total AOD was from anthropogenic emissions during pre-monsoon.

REFERENCES

Arola, A., Schuster, G., Myhre, G., Kazadzis, S., Dey, S., Tripathi, S., 2011. Inferring absorbing organic carbon content from aeronet data. Atmospheric chemistry and physics 11, 215–225.

Bessagnet, B., Hodzic, A., Vautard, R., Beekmann, M., Cheinet, S., Honore,´ C., Liousse, C., Rouil, L., 2004. Aerosol modeling with CHIMERE-preliminary evaluation at the continental scale. Atmos. Environ. 38, 2803–2817. doi:10.1016/j.atmosenv. 2004.02.034.

Bollasina, M.A., Ming, Y., Ramaswamy, V., 2011. Anthropogenic aerosols and the weakening of the south asian summer monsoon. Science, 334, 502–505.

Moorthy, K.K., Beegum, S.N., Srivastava, N., Satheesh, S., Chin, M., Blond, N., Babu, S.S., Singh, S., 2013. Performance evaluation of chemistry transport models over India. Atmos. Environ. 71, 210–225

Ganguly, D., Ginoux, P., Ramaswamy, V., Winker, D.M., Holben, B.N., Tripathi, S.N., 2009. Retrieving the composition and concentration of aerosols over the Indo–Gangetic basin using CALIOP and AERONET data. Geophys. Res. Lett. 36. doi:10.1029/ 2009GL038315.

George, S.K., Nair, P.R., Parameswaran, K., Jacob, S., 2011. Wintertime chemical com-position of aerosols at a rural location in the indo-gangetic plains. Journal of Atmospheric and Solar-terrestrial Physics 73, 1798–1809.

Kumar, D.B., Verma, S., Boucher, O., Wang, R., 2018. Constrained simulation of aero-sol species and sources during pre-monsoon season over the indian subcontinent. Atmo-spheric Research 214, 91–108.

Moorthy, K.K., Beegum, S.N., Srivastava, N., Satheesh, S.K., Chin, M., Blond, N., Babu, S.S., Singh, S., 2013a. Performance evaluation of chemistry transport models over India. Atmos. Environ. 71, 210–225. doi:10.1016/j.atmosenv.2013.01.056.

Nair, V.S., Solmon, F., Giorgi, F., Mariotti, L., Babu, S.S., Moorthy, K.K., 2012. Simulation of South Asian aerosols for regional climate studies. J. Geophys. Res. 117, D04209.

Sajani, S., Moorthy, K.K., Rajendran, K., Nanjundiah, R.S., 2012. Monsoon sensitivity to aerosol direct radiative forcing in the community atmosphere model. Journal of Earth System Science 121, 867–889

Zhang, L., Gong, S., Padro, J., Barrie, L., 2001. A size-segregated particle dry deposition scheme for an atmospheric aerosol module. Atmospheric environment 35, 549